npg

Survival, neuron-like differentiation and functionality of mesenchymal stem cells in neurotoxic environment: the critical role of erythropoietin

L Danielyan*,[1,10], R Schäfer*,[2,10], A Schulz[3], T Ladewig[4], A Lourhmati[1], M Buadze[1], AL Schmitt[1], S Verleysdonk[5], D Kabisch[1], K Koeppen[4], G Siegel[2], B Proksch[1], T Kluba[6], A Eckert[7], C Köhle[8], T Schöneberg[3], H Northoff[2], M Schwab[1,9] and CH Gleiter[1]

Mesenchymal stem cells (MSCs) can ameliorate symptoms in several neurodegenerative diseases. However, the toxic environment of a degenerating central nervous system (CNS) characterized by hypoxia, glutamate (Glu) excess and amyloid beta (Abeta) pathology may hamper the survival and regenerative/replacing capacities of engrafted stem cells. Indeed, human MSC (hMSC) exposed to hypoxia were disabled in (i) the capacity of their muscarinic receptors (mAChRs) to respond to acetylcholine (ACh) with a transient increase in intracellular $[Ca^{2+}]$, (ii) their capacity to metabolize Glu, reflected by a strong decrease in glutamine synthetase activity, and (iii) their survival on exposure to Glu. Cocultivation of MSC with PC12 cells expressing the amyloid precursor protein gene (APPsw-PC12) increased the release of IL-6 from MSC. HMSC exposed to erythropoietin (EPO) showed a cholinergic neuron-like phenotype reflected by increased cellular levels of choline acetyltransferase, ACh and mAChR. All their functional deficits observed under hypoxia, Glu exposure and APPsw-PC12 cocultivation were reversed by the application of EPO, which increased the expression of Wnt3a. EPO also enhanced the metabolism of Abeta in MSC by increasing their neprilysin content. Our data show that cholinergic neuron-like differentiation of MSC, their functionality and resistance to a neurotoxic environment is regulated and can be improved by EPO, highlighting its potential for optimizing cellular therapies of the CNS.

Cell Death and Differentiation (2009) **16,** 1599–1614; doi:10.1038/cdd.2009.95; published online 17 July 2009

The concept of stem cell therapy is based on the mainstream idea of protecting the parenchymal cells of a diseased host organ and replacing those that have already failed in their function. As candidates for the treatment of neurodegenerative diseases, bone marrow (BM)-derived mesenchymal stem cells (MSCs) possess numerous protective features as well as the capability to differentiate into functionally specialized neurons.[1] They have been successfully applied in experimental models of cerebral ischemia[2] and Parkinson's disease (PD).[3] The benefit of MSC for the therapy of PD are likely due to their capability to differentiate into dopaminergic neurons.[4] The potential of MSC may not be restricted to the generation of only one type of specialized neurons. The identification of

conditions under which they differentiate into other types of neurons would greatly enhance their potential therapeutic value.

As the successful transplantation of stem cells into a diseased organ requires their capacity not only to survive in the diseased environment but also to protect or replace host cells in their function, the response of stem cells to the pathological environment specific for the diseased host organ has to be considered. Among the common factors occurring in a broad range of neurodegenerative diseases, hypoxia and glutamate (Glu) excess have a prominent role in maintaining the pathological milieu and exacerbate the disease. Hypoxia enhances the production of amyloid beta (Abeta) and the

likelihood of developing AD.[5] Hypoxia is also widely discussed to have a role in the demyelination of axons in MS[6] and to decrease the dopaminergic activity.[7] Finally, hypoxia is known to occur after cell transplantation and to affect eminently the survival of the implanted cells in the first critical post-transplantational phase. Hypoxic preconditioning of stem cells before transplantation may improve the survival and therapeutic effects of implanted cells.[8] The role of Glu in the pathophysiology of neurodegenerative diseases mostly revolves around its excitotoxic effects as a common mechanism of neuronal damage in AD, PD, stroke, neurotrauma and MS.[9] One of the factors known to protect different types of neural cells against both hypoxia- and Glu-induced cytotoxicity is erythropoietin (EPO). Its protective and regenerative effects have been shown for a broad range of neurodegenerative diseases in both experimental and clinical trials; EPO enhances neurogenesis and provides neuroprotection during experimental stroke.[10] It exerts an anti-inflammatory effect on the central nervous system (CNS) in a model of experimental autoimmune encephalomyelitis[11] and improves motor function in MS patients.[12] The ability of EPO to prevent early and late apoptotic neuronal injury during Abeta toxicity *in vitro* raises the possibility of its therapeutic benefit during AD.[13] EPO has been recently shown to protect dopaminergic neurons and to improve neurobehavioral outcome in a rat model of PD.[14] It also abolishes hypoxia-induced death of neuronal progenitors *in vitro*[15] and acts synergistically with MSC to potentiate the post-ischemic neurogenesis in a rat model of cerebral ischemia.[16] Although these findings support a pivotal role of EPO in neuroprotection, the mechanisms of its beneficial influence on therapeutic cells (e.g., MSC) remain unclear. Taking into consideration that MSC engrafted into neurodegenerative tissue will be exposed to hypoxia (either caused by surgery or initially present as a pathogenetic factor of the respective disease) and Glu excess (caused by the disease), in this study we investigated the influence of EPO on the survival, differentiation and protective features of MSC

exposed to hypoxia, Glu and Abeta. The results of this study identify EPO as a crucial factor in the specialized cholinergic neuron-like differentiation of MSC, as well as in their acquirement of neuroprotective features such as the glutamate transporter, GLAST, and the glutamate-metabolizing enzyme, glutamine synthetase (GS). This suggests that EPO should be co-administered as a therapeutic agent in a stem cell-based therapy (CBT) of neurodegenerative disorders.

Results

Human MSC (hMSC) showed adipogenic differentiation (lipid vacuoles stained with oil red O shown in Figure 1, row a) after treatment for 21 days with adipogenic medium. After treatment for 21 days with osteogenic medium, staining for alkaline phosphatase showed osteogenic differentiation (pink color in Figure 1, row o). A 14-day long treatment with chondrogenic medium resulted in chondrocyte pellets. Alcian blue stained the mucopolysaccharides blue to bluish green (Figure 1, row c).

Under normoxic conditions (NCs), hMSC weakly expressed EPOR (Figure 2a). Most of the cells were positive for β-tubulin III. Administration of EPO under NCs led to the stronger expression of β-tubulin III (Figure 2b) and appearance of cells with neuron-like morphology (arrow in Figure 2b). Expression of EPOR was upregulated by hypoxia (Figure 2c). Application of EPO under hypoxic conditions (HCs) led to a most prominent increase in the population of neuron-like cells that formed neurosphere-like clusters and showed a strong expression of β-tubulin III and EPOR (Figure 2d).

Under normoxia, a small population of hMSC expressed glial fibrillary acidic protein (GFAP; Figure 2e). No changes in the number of GFAP-positive cells were seen in EPO-treated cultures under NC (cf. Figures 2e and f). Hypoxia changed the morphology of GFAP-positive cells: the cells were of a round, undifferentiated shape under HC in comparison with a polygonal shape under NC (cf. arrows in Figures 2g and e).
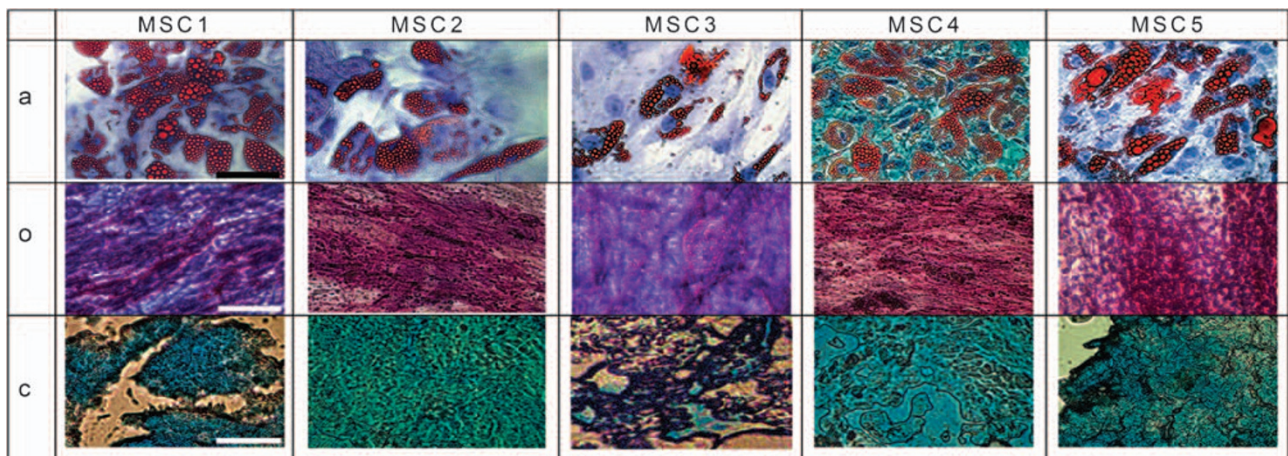
Figure 1 Light microscopy of adipogenically, osteogenically and chondrogenically differentiated adult hMSC from five donors. **a**: Adipogenic differentiation after 21 days of treatment with adipogenic medium. Staining with oil red O and hematoxylin counterstaining (scale bar: 100 μm). Red droplets represent lipid vacuoles. **o**: Osteogenic differentiation after 21 days of treatment with osteogenic medium. Staining for alkaline phosphatase and hematoxylin counterstaining (scale bar: 50 μm). Positive cells are stained pink to violet. **c**: Chondrogenic differentiation after 14 days of treatment with chondrogenic medium. Mucopolysaccharides are stained blue to bluish green (scale bar: 50 μm)
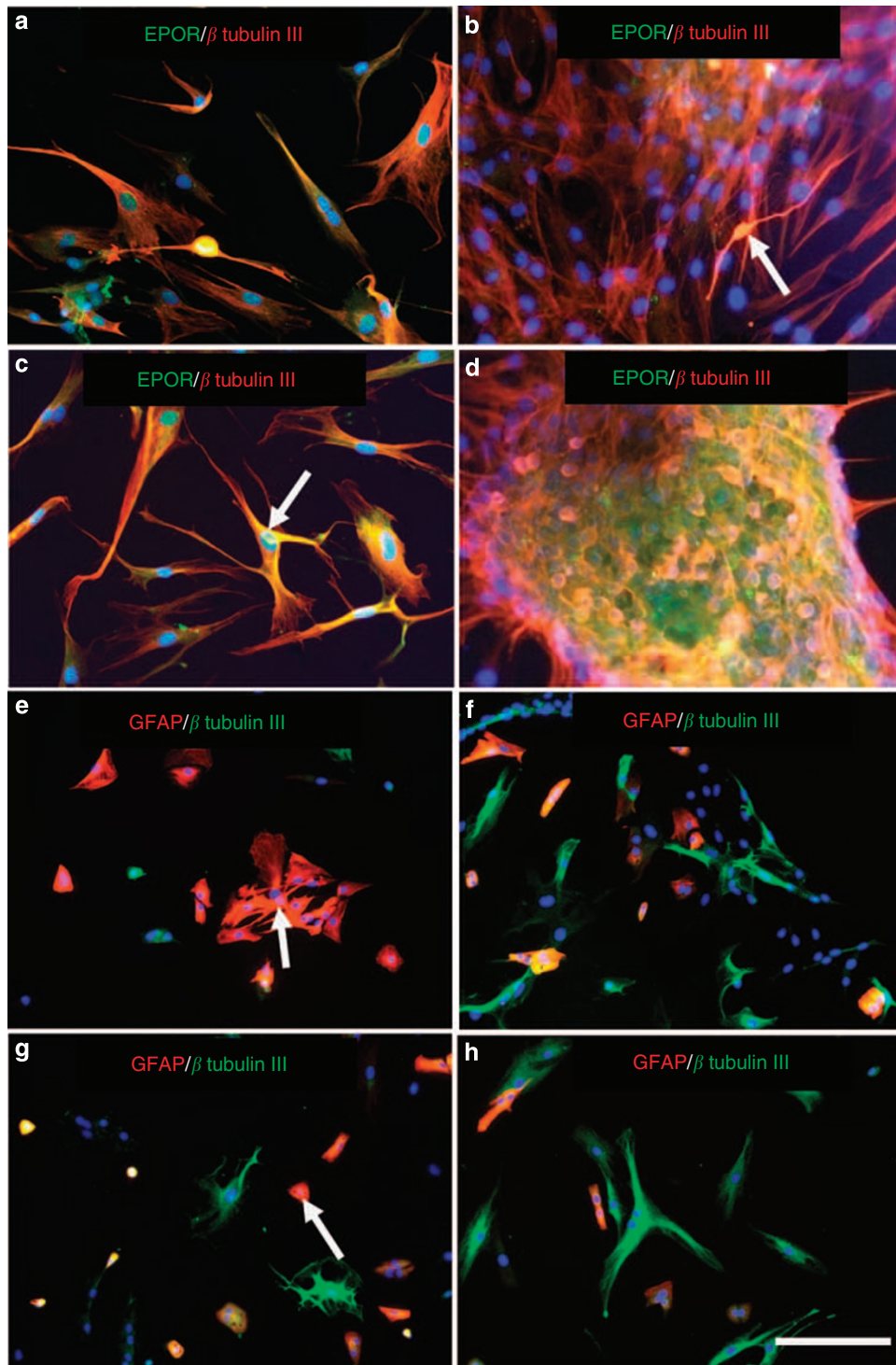
Figure 2 Expression of EPOR, β-tubulin III and GFAP in hMSC under normoxic and hypoxic conditions. EPOR (green in **a–d**) weakly expressed in normoxic control cultures (**a**) and EPO-treated hMSC under normoxia (**b**) was upregulated in hypoxic controls (**c**). The level of EPOR expression under hypoxia was not affected by EPO treatment (**d**). β-tubulin III (red in **a–d**, green in **e–f**) was expressed by the majority of cells in normoxic (**a**) and hypoxic controls (**c**), especially those expressing EPOR (arrow in **c**). Cells treated with EPO under normoxia developed a neuron-like morphology (arrow in **b**). EPO strongly increased the population of β-tubulin III-positive, neuron-like cells under hypoxic culture conditions (**d**). Only a small subpopulation of hMSC expressed GFAP in all culture conditions analyzed (red in **e–h**). EPO decreased the number of GFAP-positive cells upon hypoxic (**h**) but not normoxic (**f**) conditions in comparison with the respective normoxic (**e**) and hypoxic (**g**) controls. GFAP-positive cells possessed polygonal shapes under normoxia (arrow in **e**), but round shapes under hypoxia (arrow in **f**). The cell nuclei were stained with DAPI (blue). Scale bar: 100 μm

EPO-treated cells under HC expressed less GFAP than those in the corresponding HC control (cf. Figure 2h *versus* Figure 2g).

Analysis of EPO and GS expression in hMSC showed an intense staining for endogenously produced EPO in cells strongly expressing GS under NC (arrow in Figure 3a).
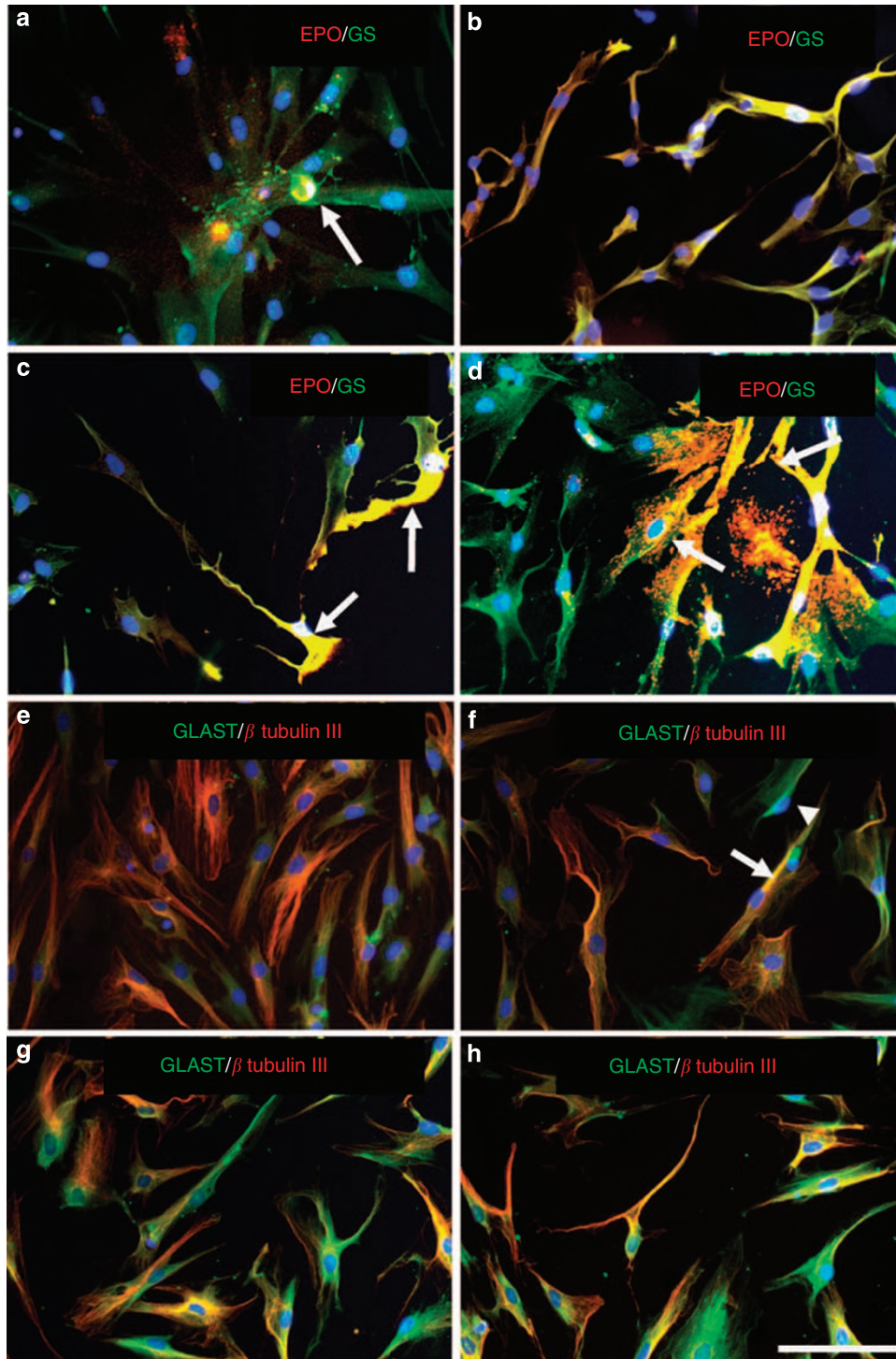
Figure 3 Influence of hypoxia and EPO on the Glu-metabolizing phenotype of hMSC. Strong expression of GS (green in **a**–**d**) coexisted with an intense staining for EPO (red in **a**–**d**) endogenously expressed under normoxic (arrow in **a**) and hypoxic (arrows in **c**) control conditions shown by intense yellow staining of cells. After application of EPO upon normoxia (**b**) and hypoxia (**d**), the majority of cells expressed GS. The most intense staining of GS was seen in EPO-positive cells (arrows in **d**). GLAST (green in **e**–**h**) was weakly expressed in β-tubulin III-positive cells in the normoxic control (**e**) and was slightly upregulated by EPO under normoxia (**f**). Hypoxia increased the number of GLAST-positive cells (**g**). The most intense staining of GLAST is seen in EPO-treated cultures upon hypoxia (**h**). The cell nuclei were stained with DAPI (blue). Scale bar: 100 μm

Application of EPO under NC increased the population of cells positive for EPO, indicating the uptake of exogenously applied EPO by hMSC (Figure 3b). These cells revealed a strong expression of GS reflected by intense yellow staining resulting from merged green (GS) and red fluorescence (EPO) in Figure 3b.

Hypoxia enhanced the endogenous expression of EPO in cells strongly positive for GS (arrows in Figure 3c). Application of EPO under HC resulted in an increase of GS staining in a majority of the cells (Figure 3d), with a most intense staining in cells strongly positive for EPO (arrows in Figure 3d).

A weak expression of GLAST (green in Figures 3e–h) was seen in cultures under NC (Figures 3e and f). GLAST was expressed in both β-tubulin III-positive MSCs (arrow in Figure 3f) and cells lacking β-tubulin III (arrowhead in Figure 3f). Hypoxia slightly increased the expression of GLAST in hMSC (Figure 3g), although the most intense staining for GLAST was observed in cultures exposed to EPO under hypoxia (Figure 3h).

Glutamate decreased the viability of hMSC under NC reflected by an increased lactate dehydrogenase (LDH) release from hMSC in comparison with a NC control without Glu (Figure 4a). Both preincubation of cells with EPO before exposure to Glu and co-administration of EPO and Glu under NC diminished the release of LDH (Figure 4a). Exposure to Glu under hypoxia showed a higher increase in LDH levels than the one seen under NC (cf. $+$G in Figure 4b with $+$G in Figure 4a). EPO given before or simultaneously with Glu was capable of increasing the viability of hMSCs to the levels of the hypoxic control without Glu (Figure 4b).

Under NC, cells exposed to Glu showed a higher activity of GS, when compared with samples incubated without Glu (Figure 4c). Application of EPO before the exposure of the cells to Glu or simultaneously with Glu led to a significant increase in GS activity under NCs. Here, cells preincubated with EPO before exposure to Glu did not reveal higher levels of GS activity in comparison with those incubated with EPO and Glu simultaneously (Figure 4c). Addition of 1 mM Glu under hypoxia did not change the activity of GS, whereas EPO, either preincubated or applied simultaneously with hypoxia and Glu, significantly increased the GS activity of hMSC (Figure 4d).

Immunofluorescence analysis revealed a weak perinuclear expression of synaptophysin in hMSC under NCs (Figure 5a). The cells exposed to EPO under NC possessed synaptophysin in cell bodies and processes (Figure 5b) and were also positive for β-tubulin III (arrows in Figure 5b). HMSC exposed to hypoxia revealed a higher expression of synaptophysin compared with that in the NC (Figure 5c), whereas the application of EPO under HC appeared to induce the formation of vesicles containing synaptophysin in the area of contact between the cells (arrowheads in Figure 5d).

The quantification of acetylcholine (ACh) in the culture supernatant of hMSC showed that Glu reduces the production/release of ACh in hMSC in comparison with the NC (Figure 5e), whereas EPO applied simultaneously with Glu restored the production of ACh to the levels of the NC-control (Figure 5e). Exposure of hMSC cultures to the soluble cysteine-rich domain (CRD) of Fzd7, a functional antagonist of Wnt3a,[17] abolished the effect of EPO on the release of ACh

(Figure 5e). Similar to the co-administration with EPO, CRD Fzd7 applied alone decreased the ACh down to the level of the control treated with Glu (Figure 5e).

The assessment of apoptosis in hMSC cultures by quantification of TUNEL-positive cells revealed a strong anti-apoptotic effect of EPO. EPO prominently decreased the number of TUNEL-positive cells upon normoxia (Figure 5f, cf. N versus N$+$EPO), hypoxia (Figure 5f, cf. H versus H$+$EPO) and exposure to Glu under both NC and HC (Figure 5f, cf. N$+$G versus N$+$G$+$EPO and H$+$G versus H$+$G$+$EPO). However, EPO could not decrease the number of apoptotic cells if combined with CRD Fzd7. In fact, under this condition the number of TUNEL-positive cells was almost eightfold higher than in the respective normoxic or hypoxic controls (Figure 5f, cf. N versus N$+$EPO$+$CRD Fzd7 and H versus H$+$EPO$+$CRD Fzd7). The number of TUNEL-positive cells was also dramatically increased in the presence of CRD Fzd7 applied alone (Figure 5f, cf. N versus N$+$CRD Fzd7 and H versus H$+$CRD Fzd7).

Exposure of hMSC to EPO under NC led to an increase in the number of neuronal nuclei-specific protein (NeuN)-positive cells (cf. Figures 6a and b and N versus N$+$E in Figure 6e). Hypoxia did not lead to significant changes in the number of NeuN-positive hMSC (Figures 6a and c, N versus H in Figure 6e). EPO applied under HC considerably increased the population of NeuN-positive hMSC (Figure 6c versus Figure 6d). The number of cells was even higher than that in normoxic control cultures (cf. H$+$E with H and N in Figure 6e). To prove that the increase in the number of NeuN-positive hMSC cannot simply be explained by the increase in the total number of cells under NC and HC conditions, either due to a proliferative effect of EPO or by its survival-increasing effect under hypoxia, we counted the total cell number by the quantification of nuclei stained with 4′,6 diamidino-2-phenylindole (DAPI). Neither under NC nor under HC could a change in cell number be observed after application of EPO (Figure 6f).

Further analyses have shown that EPO is capable of: (i) enhancing the expression of synaptophysin, ChAT, leukemia-inhibitory factor (LIF), GLAST, neprilysin, Wnt3a, β-catenin (Figure 7 and Table 1), M1-M3R and β-tubulin III (Figure 8); (ii) increasing the response of MSC to ACh shown by a transient increase in intracellular Ca^{2+} (Figure 9); (iii) decreasing the Abeta-induced release of IL-6 from MSC; and (iv) increasing the Abeta-degrading function of MSC in the presence of APPsw-PC12 cells (Figure 10). For the detailed explanation of the data shown in Figures 7–10 and Table 1 see supplementary information online.

Discussion

The data shown here reflect a strong capacity of EPO to induce neurogenic differentiation of hMSC, which is potentiated by simultaneous exposure of the cells to hypoxia. A prominent increase in expression of numerous neuronal markers (β-tubulin III, NeuN, ChAT, muscarinic M1R, M2R and M3R) was observed after treatment with EPO under both normoxic and, especially, hypoxic conditions. EPO also increased the generation of vesicles containing synaptophysin. The synergistic effect of hypoxia and EPO on the
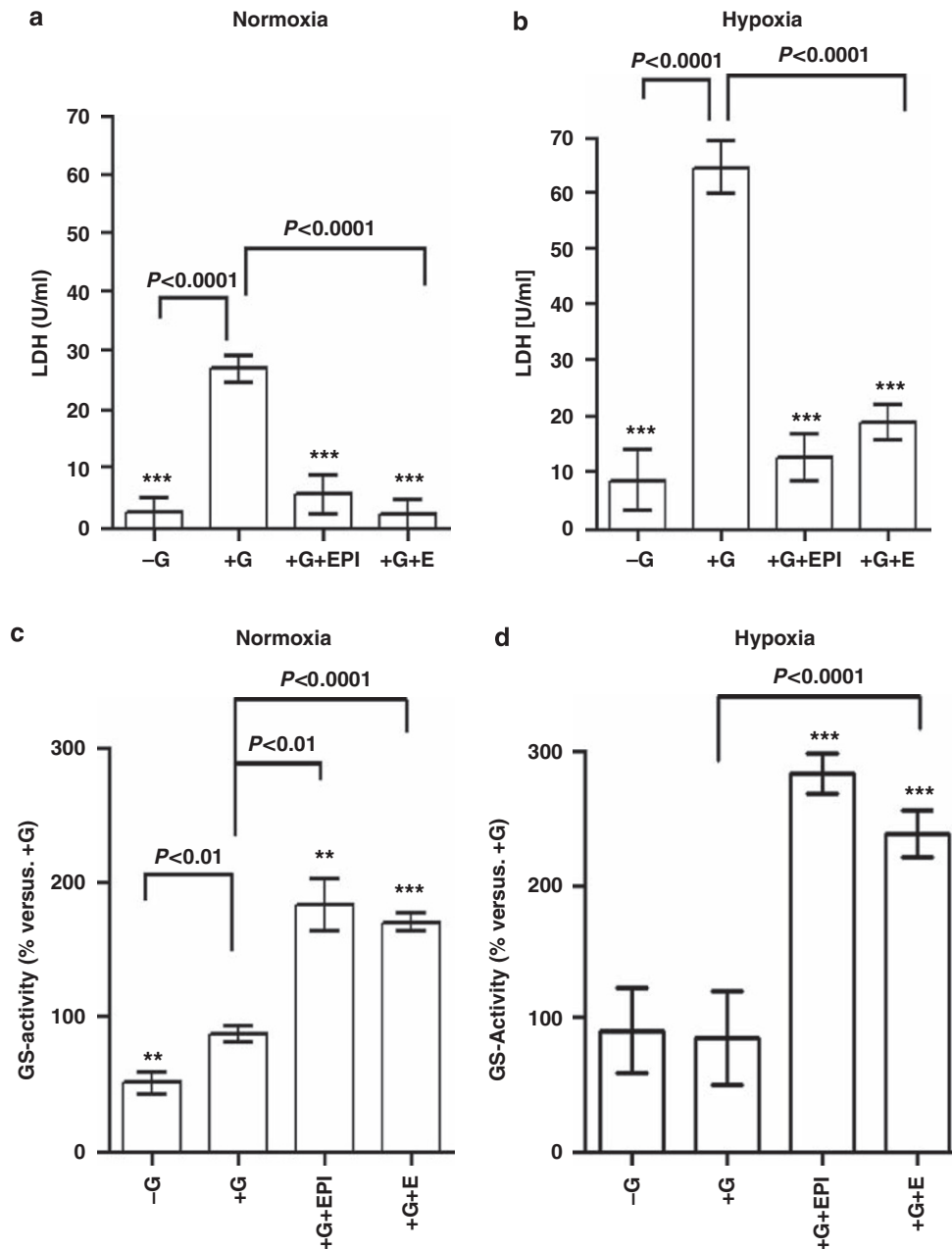
Figure 4 LDH-release and GS activity of human MSC (hMSC) under hypoxia and Glu exposure. HMSCs were cultured for 48 h under normoxic or hypoxic conditions and/or exposure to 1 mM Glu. Under normoxic conditions (**a**), 1 mM Glu increased the LDH release from cells into the culture supernatant (+G) as compared with the control without Glu (−G). EPO applied simultaneously (+G+E) or 24 h before exposure of the cultures to 1 mM Glu (+G+EPI) significantly decreased the LDH release from cells in comparison with the control exposed to Glu (+G). Hypoxia (**b**) potentiated the toxic effect of Glu on hMSC, as reflected by more LDH activity in the culture supernatant (+G) compared with the control without Glu (–G). A comparison of +G normoxia (**a**) with +G hypoxia (**b**) also reveals a highly significant difference as a consequence of Glu toxicity (2.4-fold increase of LDH under hypoxia, $P<0.0001$). EPO either co-administered with Glu (+G+E) or preincubated (+G+EPI) with the cells before Glu exposure strongly reduced the LDH-release under hypoxia. Glu (1 mM) induced GS activity in hMSC under normoxic conditions (**c**, +G) in comparison with control cultures without exposure to Glu (**c**, –G). Hypoxia (**d**) disabled hMSC in their capacity to upregulate their GS activity in response to 1 mM Glu (no difference between –G and +G in **d**). EPO applied simultaneously with exposure of cells to Glu (+G+E) under normoxic (**c**) and hypoxic (**d**) conditions enhanced the GS activity. Pretreatment of cultures with EPO did not cause an additional increase in GS activity. The data are shown as percentages (mean ± S.E.M.) of the respective controls under normoxia (**c**, +G) and hypoxia (**d**, +G). One-way ANOVA with Bonferroni's comparison was used for multiple comparisons between controls and treated samples (***$P<0.0001$, **$P<0.001$)

upregulation of neuronal (β-tubulin III, NeuN, ChAT, muscarinic M1R, M2R and M3R) and functional markers (GLAST, neprilysin) can be explained by increased EPOR synthesis in MSC under HCs. The upregulation of EPOR shown here is concordant with the report of Zwezdaryk *et al.*[18] showing the hypoxia-induced upregulation of EPOR in hMSC. EPO seems to induce neuron-like differentiation of hMSC acting synergistically with hypoxia, and at the same time may restrict glia-like
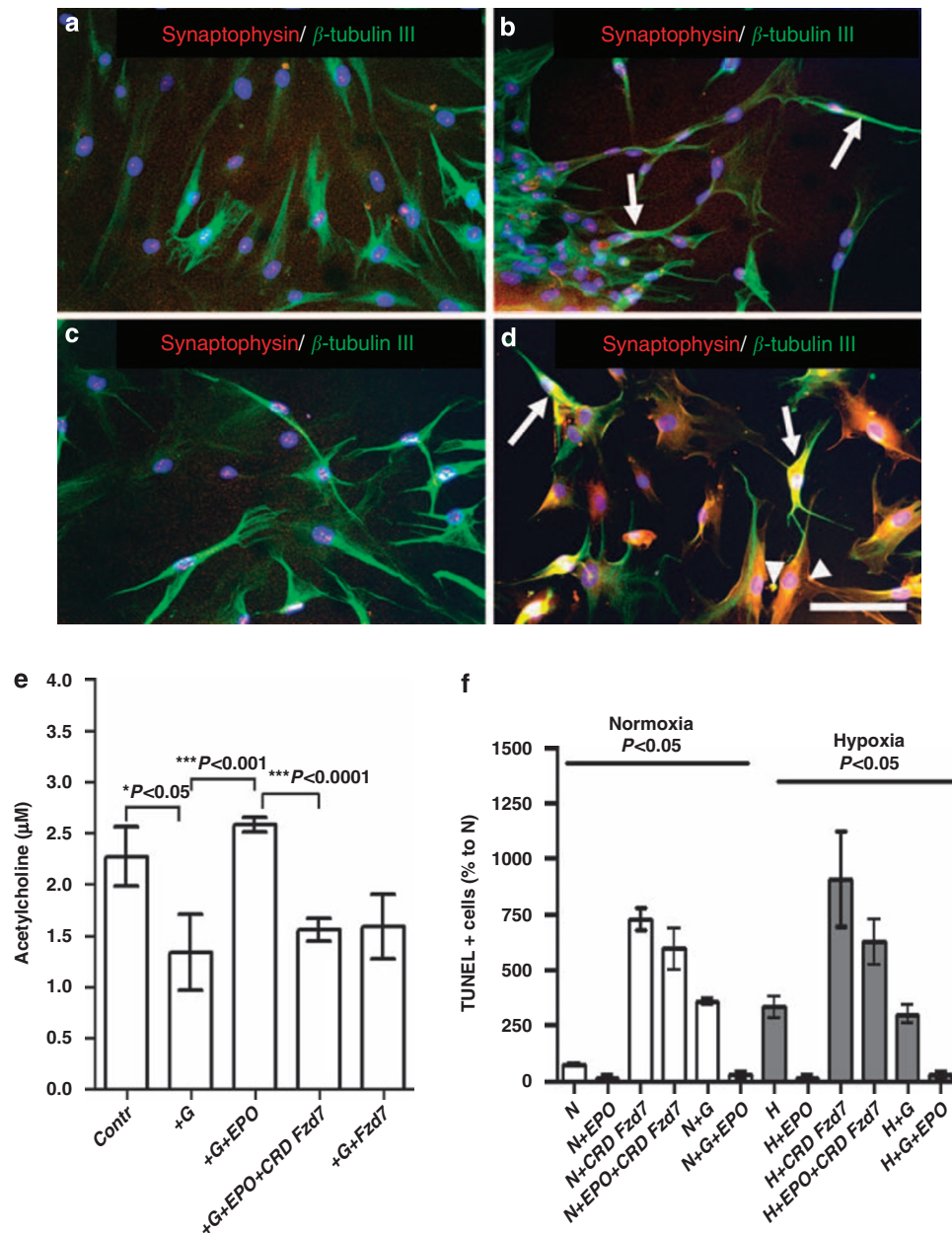
Figure 5 Detection of synaptophysin, ACh and DNA ends (TUNEL) in hMSC upon hypoxia and EPO-treatment. Synaptophysin (red in **a–d**) was weakly expressed by β-tubulin III-positive cells (green throughout **a–d**) under normoxic control conditions (**a**). A slight increase in a population of synaptophysin-positive cells was seen under EPO treatment under normoxia (arrows in **b**). Hypoxia (48 h) slightly increased the synaptophysin expression (**c**). EPO applied under hypoxic conditions led to the formation of vesicles containing synaptophysin (arrowheads in **d**). The cell nuclei were stained with DAPI (blue). Scale bar: 100 μm. Acetylcholine (panel **e**) was detected in the cell culture supernatant of hMSC cultured under normoxia and exposed to glutamate (Glu) for 48 h. The antagonist of Wnt3a signaling, CRD Fzd7, was applied at 1 h before the application of EPO and Glu (1 mM). Glu (+ G in **e**) reduced the release of ACh in hMSC (cf. control with + G in **e**, $P < 0.03$), whereas the application of EPO to Glu-exposed cultures enhanced the levels of ACh (cf. + G versus + G + EPO, $P < 0.001$ in **e**). CRD Fzd 7 abolished their effect of EPO (cf. + G + EPO with + G + EPO + CRD Fzd7, $P < 0.0001$ in **e**). The data are shown as mean ± S.E.M. One-way ANOVA with Bonferroni's comparison was used for multiple comparisons between controls and treated samples. Quantification of TUNEL + cell was performed in hMSC cultures exposed to hypoxia (48 h), 1 mM Glu and CRD Fzd7 (preincubated for 1 h before the application of EPO). The data are shown in percentages (mean ± S.E.M.) of the normoxic control (N in panel **f**). One-way ANOVA with Bonferroni's comparison was used for multiple comparisons between control and treated samples (***$P < 0.0001$, **$P < 0.001$)

differentiation of MSC. The decrease in the number of GFAP-positive cells under hypoxia and EPO administration cannot be simply explained by cellular death, as EPO has been shown to protect hMSC from hypoxia-induced cell death and/or Glu toxicity (shown by TUNEL quantification). Here we also show that hMSC produce GS, the activity of which seems to be upregulated by EPO. In the CNS, GS is physiologically produced by astrocytes and has a pivotal role in the
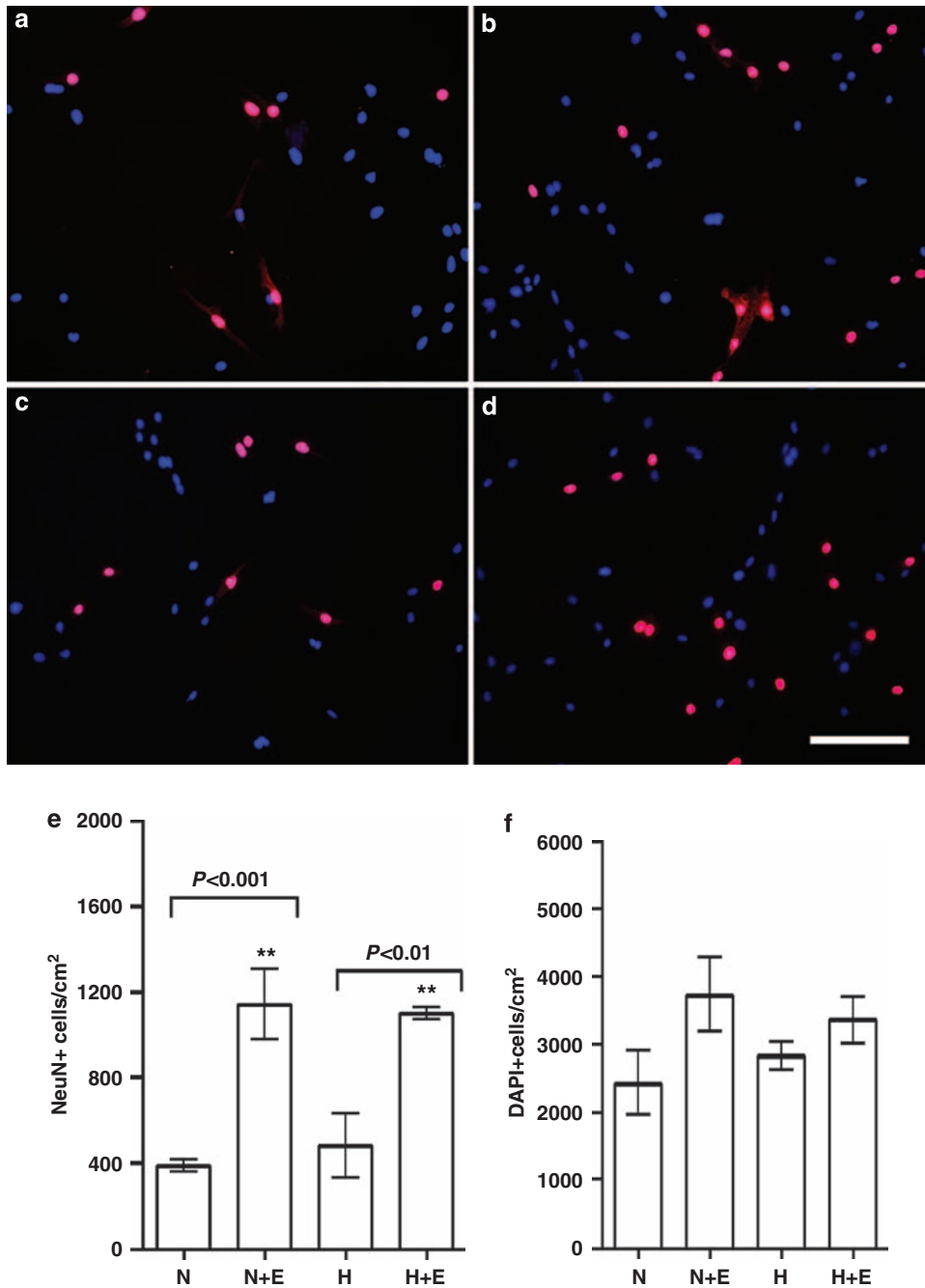
Figure 6 NeuN-positive population of hMSC under hypoxia and treatment of EPO. NeuN-positive cells (red and pink staining resulting from merged bluish DAPI and red NeuN staining) were detected under normoxic (**a**) and hypoxic (**c**) control conditions. Treatment with EPO increased the number of NeuN-positive cells under normoxic (**b**) and hypoxic (**d**) condition. Scale bar: 100 μm. Quantification of NeuN-positive hMSC (**e**) revealed an increase in the number of NeuN-positive cells in cultures supplemented with EPO under normoxic (N + E) and hypoxic (H + E) conditions in comparison with the respective controls (N and H). The total amount of cells evaluated by quantification of DAPI-positive cells remained unchanged either after exposure of cells to hypoxia or application of EPO (**f**). Data presented as mean ± S.E.M. were analyzed by Student's *t*-test comparing each treated sample with its respective control

glutamine–glutamate cycle. This cycle assures the removal of excitotoxic concentrations of Glu from the extracellular space and therefore the survival of neurons. However, under pathological conditions such as ischemia and AD, astrocytes are hampered in their capacity to produce GS, whereas neurons start to synthesize this enzyme.[19] HMSC exposed to hypoxia failed to respond to 1 mM Glu with an increase in GS activity, reflecting the inability of hMSC to survive and maintain their Glu-metabolizing function on simultaneous exposure to hypoxia and Glu. EPO decreased LDH release from hMSC down to the levels of the respective hypoxic but Glu-free control and induced GS activity. It has been shown

Table 1 Densitometric values of proteins analyzed in hMSC by western blot shown in Figure 7

Protein	N	Condition						
		N+EPO	N+CRD Fzd7	N+EPO+CRD Fzd7	H	H+EPO	H+CRD Fzd7	H+EPO+ CRD Fzd7
		% to normoxic control (N)						
Synaptophysin	100	324	171	160	299	498	291	334
ChAT	100	169	34	47	156	226	22	52
LIF	100	194	105	149	193	246	206	176
EPOR	100	135	111	122	223	119	104	72
GFAP	100	109	254	257	237	168	216	156
GLAST	100	259	84	110	142	223	63	77
Neprilysin	100	148	37	52	92	161	54	88
Wnt3a	100	169	49	95	348	510	51	41
β-catenin	100	93	72	80.7	59	97	45	71

The values are indicated in % of the respective normoxic control value of each target protein
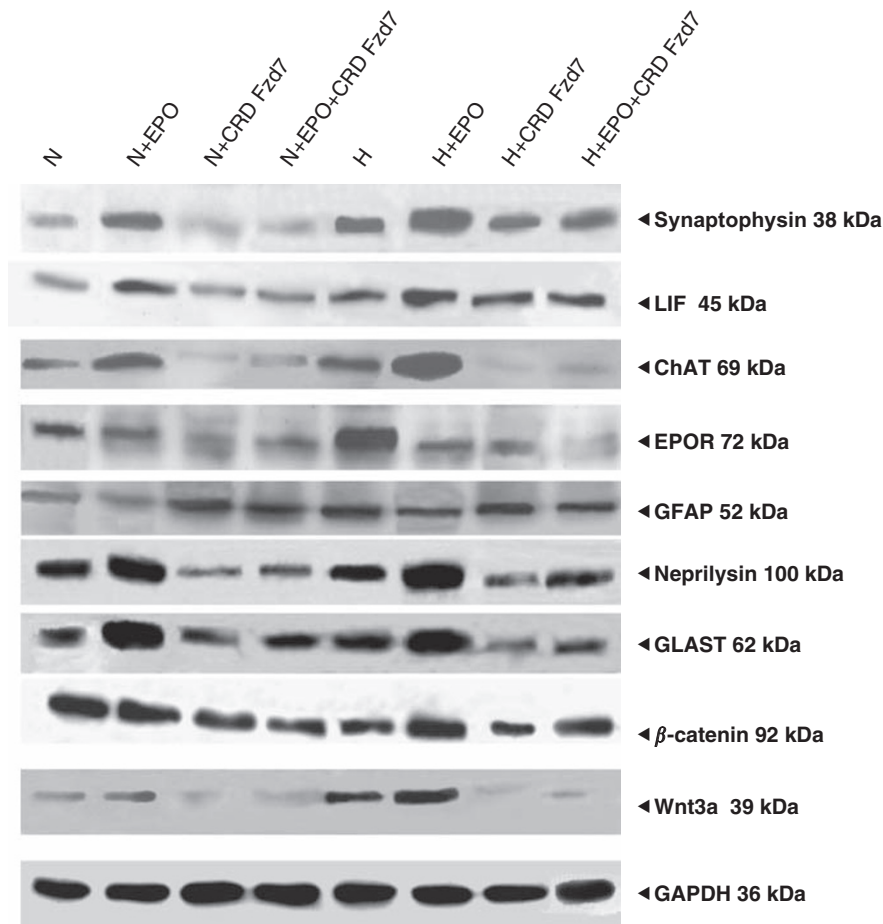
Figure 7 Western blot analysis of Wnt3a, β-catenin, neprilysin, LIF, GLAST, glial and synaptic markers in hMSC upon hypoxia and EPO treatment. Samples from normoxic (N) and hypoxic (H) controls, from EPO-treated cultures (N + E and H + E) and from cultures treated with EPO in the presence of CRD Fzd7 (N + EPO + CRD Fzd7 and H + EPO + CRD Fzd 7) were analyzed for the presence of synaptophysin, LIF, ChAT, EPOR, GFAP, neprilysin, GLAST, β-catenin and Wnt3a. GAPDH was used as a loading control

previously that *in vitro*, MSC express GS and the Glu transporters GLAST and GLT-1,[20] indicating that these cells may be able to take over the Glu-metabolizing function of astrocytes. Our data confirm that MSC do not only produce the active enzyme (GS) and GLAST, but they can also effectively take up Glu *in vitro* (unpublished results). We also show that without EPO hMSC exposed to hypoxia cannot increase their GS activity in response to Glu excess, whereas EPO can induce GS activity and the expression of GLAST in hMSC under these toxic conditions. The importance for *in vivo*
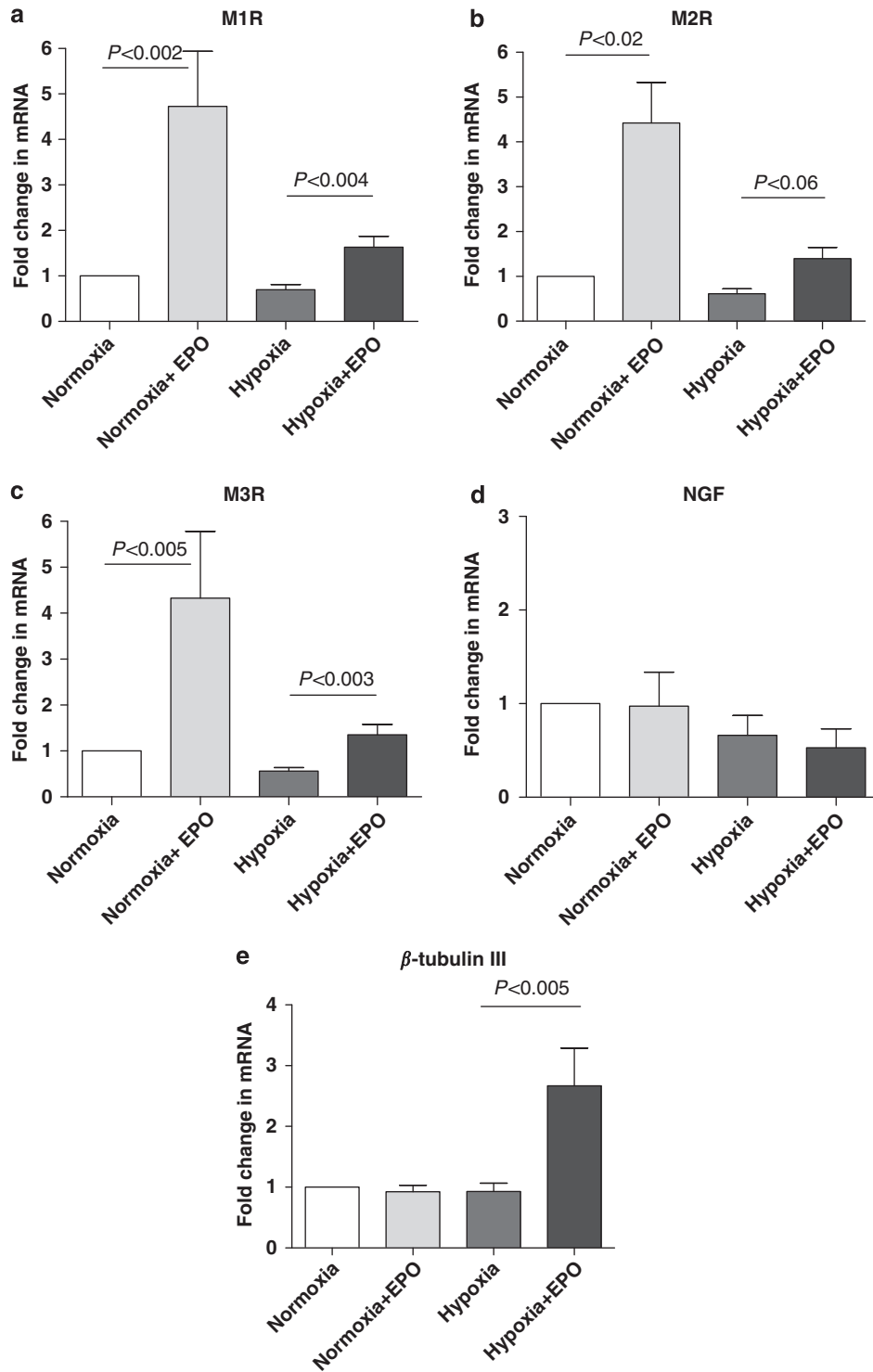
Figure 8 mRNA levels for muscarinic receptors, NGF and β-tubulin III in hMSC. Levels of the mRNAs for muscarinic receptors M1R (**a**), M2R (**b**), M3R (**c**) and of NGF (**d**) in hMCS were measured by qPCR. ΔC_T values for each transcript under the indicated conditions were calculated relative to the respective β_2-microglobulin transcript level (housekeeping transcript), and fold changes in C_T values ($\Delta\Delta C_T$ values) were computed in relation to cells cultivated under normoxic conditions. The mean C_T of the β_2-microglobulin transcript was 18.15 ± 0.68 and no differences in this value between culture conditions were seen. The change in β-tubulin III mRNA level was calculated with respect to the mean of the normoxic control (**e**). The means of five readings of independent samples are shown $\pm$ S.E.M. The experiment was carried out in duplicate. Student's *t*-test was used to compare values with their respective controls (normoxic *versus* hypoxic conditions)
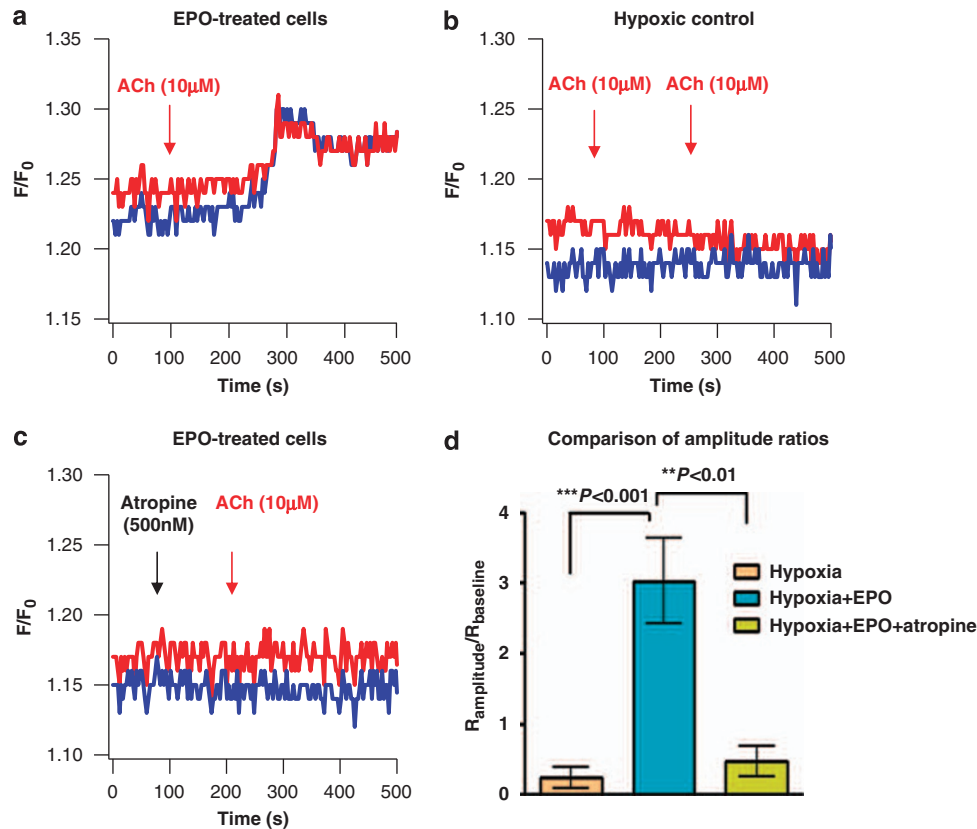
Figure 9 Intracellular Ca^{2+} transients in hMSC induced by ACh upon hypoxia and application of EPO. Fura-2-loaded hMSC treated with EPO (**a** and **c**) and from hypoxic controls (**b**) were exposed to ACh (10 μM for 30 s) in calcium-imaging experiments (F/F_0 in **a**–**c** is the ratio of Fura-2 fluorescence at 353 and 390 nm). The majority of cells (two representative measurements out of 16 in total, each colored trace represents the calcium signal of a single cell) treated with EPO upon hypoxia responded to ACh with an increase in their cytosolic Ca^{2+} concentration (**a**). MSC from control cultures exposed to hypoxia showed a strongly reduced functionality of muscarinic receptors reflected by unaltered cytosolic Ca^{2+} levels after stimulation with ACh (**b**). In control experiments, atropine was used to block the effect of muscarinic receptors in EPO-treated cells (**c**). Comparison of the amplitude ratios (the ratio of the Ca^{2+} level amplitude after stimulation with ACh was correlated to the ratio of the baseline Ca^{2+} level measured immediately before the application of ACh, $R_{amplitude}/R_{baseline}$) shows a significantly higher Ca^{2+} level amplitude after stimulation with ACh in EPO-treated cells (**d**, hypoxia + EPO) in comparison with the hypoxic (**d**, hypoxia) and the atropine-treated control (**d**, hypoxia + EPO + atropine)

transplantations of the ability of cultured differentiated MSC to maintain their phenotype and functionality under HCs prevalent in neurodegenerative disorders becomes clear when one considers the organ-specific values for oxygen partial pressure (pO_2), a major trigger for systemic EPO release (Table 2). The pO_2 levels vary considerably between the compartments alveoli, blood and the individual tissues.[21–23] As confirmed by our study, low pO_2 has been shown to promote neurogenic differentiation of MSC. However, despite its capacity to induce neurogenic differentiation, the relatively low pO_2 in the brain (in comparison with BM) can reduce the protective capacities of MSC and their survival. This negative effect of the low brain pO_2 on MSC can be further potentiated by a transplantation procedure or by neurodegenerative disorders accompanied by brain hypoxia.

AD is characterized by progressive loss of cognition, reduction of ACh and ChAT levels, as well as by loss of cholinergic innervation in the CNS. Muscarinic acetylcholine receptors are known to have a key role in the processes of cognition. Impairment of muscarinic receptor signaling (especially through M1R) is directly involved in the pathology of Alzheimer's-like disorders.[24] Moreover, M1R has a prominent role in the amyloidogenic processing of amyloid precursor protein (APP).[25] A CBT in AD will therefore be aimed at replacing damaged or lost cholinergic neurons to improve cholinergic signal transduction in the host CNS tissue. The involvement of hypoxia in AD pathology is widely discussed in recent reports. It is even proposed that mild or moderate AD may be a toxic manifestation of a primarily hypoxic disease.[26] Our data show an EPO-induced increase in production of ACh as well as expression of ChAT, M1R, M2R and M3R in hMSC. The functionality of muscarinic receptors reflected by their responsiveness to ACh and mediation of an increase in cytosolic Ca^{2+} seems to be positively affected by EPO under HCs. Expression of functional M2 receptors in MSC under NCs was reported recently by Hoogduijn et al.[27] However, besides detection of M2 receptor mRNA, these authors showed that none of the other muscarinic receptor types (M1, M3-5) could be detected on the mRNA level. Here we show an upregulation of M1-M3 receptors at the mRNA level in hMSC treated with EPO upon normoxia and hypoxia. The functional activity of M1, M3 and M5 receptors reflected by
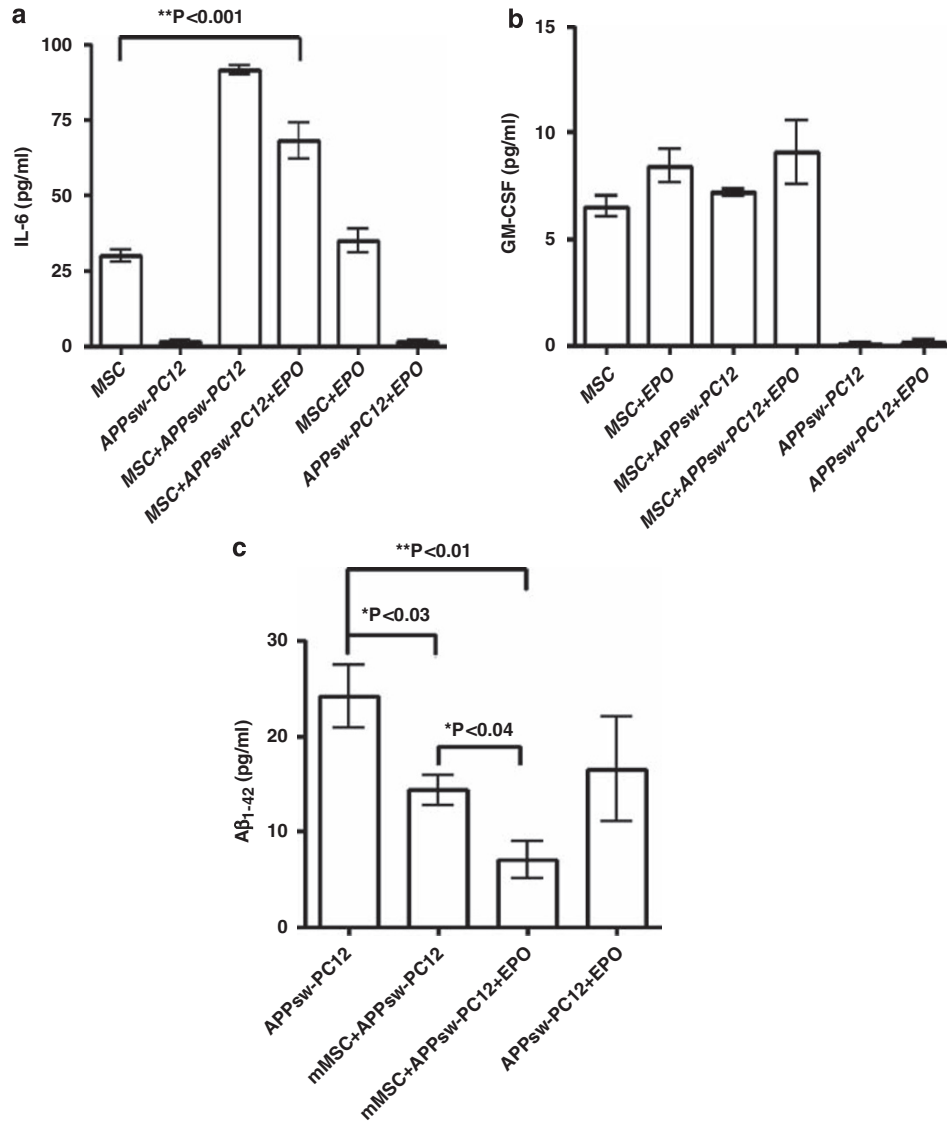
Figure 10 Multiplex analysis of cytokines released from murine (m) MSC co-cultured with APPsw-PC12. The release of IL-6 (**a**) is threefold higher in co-cultures (MSC + APPsw-PC12) than those in control monocultures (MSC). EPO applied to co-cultures (MSC + APPsw-PC12 + EPO) significantly decreased the release of IL-6 (**P<0.001, one-way ANOVA). IL-6 concentration in cell culture supernatants from monocultures of mMSC was not altered by application of EPO (cf. MSC *versus* MSC + EPO). Quantification of GM-CSF (**b**) did not show any changes in mono and co-cultures of MSC with APPsw-PC12 either in controls or in EPO-treated cultures. The quantification of Abeta$_{1-42}$ by ELISA in the cell culture supernatants (panel **c**) revealed that cocultivation of APPsw-PC12 with mMSC decreases the Abeta$_{1-42}$ concentration (cf. APPsw-PC12 with mMSC + APPsw-PC12 in **c**). EPO additionally reduces the amount of Abeta$_{1-42}$ (cf. mMSC + APPsw-PC12 *versus* mMSC + APPsw PC12 + EPO in **c**) in co-cultures but not in monocultures of APPsw-PC12 (cf. APPsw-PC12 + EPO *versus* APPsw-PC12 in c). One-way ANOVA with Bonferroni's comparison was used for multiple comparisons between control and treated samples

Table 2 Oxygen partial pressure in gas, blood and tissues

Compartment	Oxygen partial pressure (reference)
Dry atmospheric air	159 mm Hg[19]
Alveolar gas	100 mm Hg[19]
Arterial blood	95 mm Hg[19]
Mean capillary blood	45 mm Hg[19]
Bone marrow	55 mm Hg[20]
Brain tissue (7–12 mm below dura mater)	33 mm Hg[21]
Brain tissue (12–17 mm below dura mater)	33 mm Hg[21]
Brain tissue (17–22 mm below dura mater)	26 mm Hg[21]
Brain tissue (22–27 mm below dura mater)	24 mm Hg[21]

their ability to mobilize intracellular calcium is associated with stimulation of phospholipase C, which in turn leads to the release of inositol-1,4,5-triphosphate (IP$_3$) and consequently of Ca^{2+} from intracellular stores into the cytosol. M2 and M4 receptors are primarily known to inhibit adenylyl cyclase activity and to reduce the concentration of cAMP. However, they were also shown to have a stimulatory effect on phospholipase C in some cell types.[28] A transient increase of cytosolic [Ca^{2+}] in response to ACh in EPO-treated hMSC is most likely mediated through M1R and M3R with consequent activation of phospholipase C and IP$_3$ release.

Regarding the question which mechanisms are involved in induction and maintenance of the neuron-like phenotype of

MSC, we hypothesized that EPO could either (i) enhance the production of other growth factors, such as NGF or LIF, which are known to induce neuron-like differentiation in stem cells of different origin[29,30] and/or (ii) activate directly the signaling systems such as the Wnt pathway that orchestrate the growth and differentiation fate of stem cells.[31] NGF message levels remained unchanged in EPO-treated hMSC. Unlike NGF, LIF was upregulated by EPO under both normoxic and, most prominently, under HCs. LIF was recently shown to be upregulated in the ischemic brains and neural cultures exposed to oxygen/glucose deprivation.[32] This hints at the possible induction of neuron-like differentiation of implanted MSC by LIF overexpressed in ischemic brain tissue.

A recent report showed that hypoxia suppresses Wnt signaling and β-catenin activation.[33] Here we show that EPO induces the production of Wnt3a in hMSC under normoxic and, especially, hypoxic conditions. Moreover, this induction of Wnt3a by EPO under hypoxia was completely abolished by CRD-Fzd7, which is known to inhibit the activity of Wnt3a and to reduce the accumulation of β-catenin.[17] Keeping in mind that EPO also upregulates the expression and functionality of M1R, it is possible that a cross talk between muscarinic and Wnt signaling underlies the neuroprotective effect of M1R activation through the inhibition of glycogen-synthase-kinase-3β activity and stabilization of the cytoplasmic and nuclear β-catenin[34] by which the shutdown of the Wnt pathway induced by Abeta toxicity is reversed.

In addition, Wnt signaling (especially through Wnt3a) inhibits the osteogenic differentiation of hMSC.[35] Our results show that EPO-induced upregulation of ChAT, neprilysin, GLAST and LIF in hMSC upon hypoxia was abolished by CRD Fzd7. The effect of EPO on the ACh production by hMSC exposed to Glu was also sensitive to CRD Fzd7, which decreased ACh to the levels of the control. Presumably, EPO can stabilize the phenotype of neuron-like differentiated hMSC by increasing the production of Wnt3a, which in turn may prevent hMSC reprogramming. The better survival of EPO-treated hMSC on exposure to Glu and/or hypoxia may also be interconnected with Wnt3a activity. CRD Fzd7 abolished the anti-apoptotic effect of EPO under these neurotoxic conditions, as shown by quantification of TUNEL-positive hMSC. The eightfold increase in TUNEL-positive cells on application of CRD Fzd7 either alone or in combination with EPO under normoxia or hypoxia may implicate an EPO-independent role of Fzd7 signaling in hMSC survival.

The possible therapeutic use of hMSC in AD depends on the resistance of the engrafted MSC to the toxic effects of Abeta. The cocultivation of mMSC with Abeta$_{1-42}$ and Abeta$_{1-40}$-producing rat APPsw-PC12 cells resulted in enhanced release of IL-6 from mMSC. The toxic effect of Abeta on the CNS cells is reflected by cell death[36] and an inflammatory response.[37] The release of IL-6 from mMSC in response to the exposure toward Abeta produced by APPsw-PC12 cells is significantly reduced by application of EPO. The production of granulocyte-monocyte colony-stimulating factor (GM-CSF) by mMSC was not affected by cocultivation with APPsw-PC12; the concentration of GM-CSF was at a very low level, nearly equal to the basal levels of control cultures. Our data are concordant with previous studies reporting the decrease of IL-6 production in organ-specific cells and

tissues in various disease models in response to EPO.[38,39] As GM-CSF can be upregulated by Abeta,[37] and in turn may increase the production of Abeta,[40] our data suggest that engrafted MSC most likely will not harm the host tissue by additionally increasing the local GM-CSF levels. Moreover, our data show that EPO is capable of not only decreasing the inflammatory response of MSC to Abeta, but also enhances the ability of MSC to take up Abeta$_{1-42}$. This result can be explained by the capacity of MSC to express neprilysin, a major Abeta-degrading enzyme of the brain.[41] This effect of EPO seems to depend on the Wnt signaling pathway, as CRD Fzd 7 completely abolishes it under normoxia and hypoxia.

Our study points out the pivotal role of EPO in survival, functionality (electrophysiological features, expression of cholinergic and synaptic markers) and protective features (Glu-metabolizing activity) of hMSC under neurotoxic conditions characterized by hypoxia, Glu excess and the presence of Abeta that occur in a variety of neurodegenerative diseases. In MSC-based therapeutical approaches against neurodegenerative disorders, it should be kept in mind that the resistance of MSC to the pathological environment and their regenerative/replacing capacities can be improved by co-administration of EPO.

Materials and methods

BM preparation. Our study was approved by the institutional review board (ethical committee) of the University of Tübingen. BM was taken under sterile conditions from five donors (two female, three male, age: 16–74 years, no metabolic or neoplastic diseases) with informed consent during orthopedic operations: From each donor, 5 ml of whole BM was collected in a sterile heparinized syringe. From each donor the hMSC were isolated, characterized and included into the study as a separate hMSC population. The results are given as means ± S.E.M. of the recorded data from each hMSC population.

Isolation of hMSC and cell culture. To isolate hMSC from whole BM, we used the density gradient technique as previously described.[42] Briefly, 5 ml BM was resuspended in 10 ml phosphate-buffered saline (PBS) (Cambrex Bio Science, Verviers, Belgium) and laid over 15 ml Lymphoflot (sodium diatrizoate 9.1% (w/v), Ficoll 5.7% (w/v); Biotest AG, Dreieich, Germany). After centrifugation (20 min at 1000 × g, rotor brake off), the mononuclear cells were harvested, washed twice with PBS, transferred to a 75-cm² culture flask (Corning Inc., Schiphol-Rijk, the Netherlands) and incubated (37°C, 95% humidified air, 5% CO₂) with α-MEM (PAA, Cölbe, Germany), containing desoxyribonucleotides, ribonucleotides and 'ultra glutamine 1' (all from Lonza, Wuppertal, Germany), 100 IU/ml penicillin (Lonza), 100 μg/ml streptomycin (Lonza) and 10% heat-inactivated fetal calf serum (FCS) (Cambrex Bio Science). After 24 h, the non-adherent cells were removed and the adherent cells were cultured and characterized.

Basic characterization of hMSC by in vitro differentiation and FACS analysis. Mesenchymal stem cells are functionally characterized by in vitro differentiation assays.[43] We evaluated the basic differentiation potential into three mesenchymal lineages: adipogenic, osteogenic and chondrogenic differentiation. The different hMSC populations were each treated either with adipogenic medium, osteogenic medium or normal medium (control) for 21 days, as previously described[44] (modification: no addition of amphotericin B).

Adipogenic differentiation was performed using a commercially available differentiation kit (Lonza). A total of 1 × 10⁶ cells per cm² were seeded and cultured in normal medium. Reaching subconfluency, the medium was changed to adipogenic differentiation medium or control medium and the cells were cultured for 3 weeks. Thereafter, the cells were stained with oil red O for visualization of in vitro adipogenesis. For staining, after removal of the medium and washing twice with PBS, 2 ml of 10% formalin were added followed by an incubation time of 30 min. After removing the formalin and washing the cell layer with sterile water, 2 ml of isopropanol (60%, BioWhittaker, Verviers, Belgium) were added and kept for 2 min. The isopropanol was removed and 2 ml of a filtered working solution of oil red O

(three parts oil red O stock solution (300 mg oil red O powder (Sigma, Taufkirchen, Germany) + 100 ml 99% isopropanol (Sigma)) + three parts deionized water) were pipetted onto cells and left there for 5 min. Thereafter the plate was rinsed with tap water and the cells were counterstained with 2 ml hematoxylin (Sigma) for 1 min.

Osteogenic differentiation was performed using osteogenic medium containing normal medium with 10^{-8} M dexamethasone (Sigma), 0.2 mM ascorbic acid (Sigma) and 10 mM β-glycerolphosphate (Sigma). Reaching subconfluency, cells were incubated in osteogenic differentiation or control medium for 3 weeks. The osteogenic differentiated cells as well as control cells were cytochemically stained for alkaline phosphatase using a commercial staining kit according to the manufacturer's (Sigma) recommendations; after removal of the medium and washing twice with PBS, 2 ml citrate fixative (12.5 ml citrate solution + 32.5 ml acetone + 4 ml 37% formaldehyde) were added for 1 min, followed by staining with 2 ml alkaline dye (0.5 ml sodium nitrite + 0.5 ml FRV-alkaline solution + 22.5 ml deionized water + 0.5 ml naphtole AS-BI alkaline solution) for 30 min. The cell layer was washed twice and counterstained with 2 ml hematoxylin (Sigma) for 1 min.

Chondrogenic differentiation was performed using a commercially available mesenchymal functional differentiation kit (Lonza). The MSCs were treated with the chondrogenic differentiation procedure; 250×10^3 cells were transferred into a 15 ml tube. After centrifugation ($200 \times g$), 0.5 ml chondrogenic differentiation medium were added and replaced every 3–4 days. The cell suspension was cultured in the tube forming a solid pellet. After 14 days, the chondrocyte pellet was removed, squeezed on a glass slide and stained with 1% Alcian Blue 8GX (Serva, Heidelberg, Germany) in 3% acetic acid (pH 2.5).

FACS analysis was carried out with a FACScan instrument (BD Biosciences, San Jose, CA, USA) using BD CellQuest Pro software. At subconfluency (1×10^6 cells), the cells were detached from flasks at subconfluency with trypsin/EDTA (Lonza) and washed with PBS. Each sample contained a cell suspension with 5×10^5 cells in FACS buffer (PBS + 1% bovine serum albumin (Sigma) + 0.1% FCS (Lonza)). The PE-conjugated antibody (Anti-human-CD14, -CD29, -CD34, -CD43, -CD44, -CD45, -CD59, -CD73, -CD90, -CD105, -CD106, -CD117, -CD133, -CD146, -CD166, HLA class I, HLA class II) was added. After an incubation time of 20 min and two washing steps, the sample was ready for analysis. All antibodies were from BD Biosciences.

The hMSC showed the following surface epitope pattern (FACS analysis): negative for CD14, CD34, CD43, CD45, CD133 and HLA class II, and positive for CD29, CD44, CD59, CD73, CD90, CD105, CD106, CD117, CD146, CD166 and HLA class I (data not shown).

Exposure to hypoxia, Glu, EPO and CRD Fzd7. For the experiments on neurogenic differentiation of hMSC, cells were cultured in Dulbecco's modified Eagle's medium (DMEM) supplemented with 10% FCS, 100 U/ml penicillin, 100 μg/ml streptomycin and 100 mM pyruvate (supplemented DMEM, Biochrom, Berlin, Germany). Cultures were maintained at 37°C under NCs in a humidified atmosphere of 90% air and 10% CO_2. HMSCs were expanded and processed for immunocytochemistry, qPCRs, western blots, GS activity and determinations of Abeta$_{1-42}$, ACh and LDH after the third passage.

Before all measurements described below, the culture medium was removed and replaced by DMEM with or without 5 U/ml human recombinant erythropoietin (Neorecormon, Hoffmann-La Roche, Grenzach-Wyhlen, Germany) and/or Glu (1 mM). For the experiments involving Wnt pathway blockade, the CRD of mouse Frizzled-7 (Fzd7) was used (R&D systems, Wiesbaden-Nordenstadt, Germany). Mouse Fzd7 shares 99% identity with the human ortholog in the CRD. Preincubation with CRD Fzd7 (500 ng/ml) alone was performed for 1 h before the medium containing Glu and EPO was added, and the incubation was continued for another 48 h. To evaluate the effect of these additives under NC and HC, one set of the cultures was incubated at 10% CO_2 in air (normoxia), the other set was incubated at 10% CO_2 and 1% O_2 in N_2 (hypoxia) for 48 h at 37°C.

Determination of cytotoxicity. For determination of cell viability and cytotoxic effects of hypoxia and/or Glu on hMSC, the cells were cultured in 96-well plates. LDH in the cell culture supernatant was measured by the CytoTox 96 Non-Radioactive Cytotoxicity Assay (Promega, Mannheim, Germany). To determine LDH, 50 μl of the supernatant of each well were transferred to a separate assay plate, mixed with 50 μl substrate mix and incubated for 30 min at room temperature (RT). The enzymatic conversion of a tetrazolium salt into a red formazan product was stopped by adding 50 μl stop solution, and the absorbance was recorded at 490 nm in a 96-well plate reader (Sunrise, Tecan, Crailsheim, Germany). Quantification was carried out by external standardization with LDH activities in

the range between 0–800 U/ml in DMEM (standard supplied in the test kit). The absorbance value of a culture medium control was used to normalize the values obtained from the samples.

Quantification of ACh in the cell culture supernatant of hMSC. For quantification of ACh, hMSCs were cultured in 96-well plates using choline-free HBSS (H 8264, Sigma) supplemented with 10% FCS, 100 U/ml penicillin, 100 μg/ml streptomycin and 100 mM pyruvate. A 100 μl aliqot of cell culture supernatant was used and measured with the AmplexRed Acetylcholine/ Acetylcholineesterase Assay Kit (A12217, Molecular Probes/Invitrogen, Carlsbad, CA, USA) according to the manufacturer's manual. In brief, in this assay ACh is monitored indirectly using 10-acetyl-3,7-dihydroxyphenoxazine (Amplex Red Reagent), a sensitive fluorogenic probe for H_2O_2, an end product of oxidized choline. First, acetylcholinesterase converts ACh to choline, which is in turn oxidized by choline oxidase to betaine and H_2O_2. The latter reacts with the Amplex Red reagent in a 1 : 1 stoichiometry to generate the fluorescent product resorufin. Fluorescence was monitored in a fluorescence plate reader (GENios Plus, Tecan) using 550 nm for excitation and 595 nm for emission after 1 h of incubation with the reaction mix. A standard curve was prepared in the range of 0–100 μM and assayed simultaneously with the samples. Data were corrected for background fluorescence by subtracting the values derived from an ACh-free control.

Multiplex analysis of cytokine release from co-cultures of murine (m) MSC and rat PC12 overexpressing the human APP gene bearing the Swedish mutation. Before cocultivation, rat APPsw-PC12 (PC12SWQ8) cells were cultured in DMEM with 10% FCS, 5% horse serum, 100 U/ml penicillin, 100 μg/ml streptomycin, 100 mM pyruvate and G-418-BC (Biochrom), whereas mMSC isolated from the BM of three female mice (age: 6 weeks) were cultured with α-MEM (BioWhittaker) supplemented with 10% FCS (Lonza) and antibiotics/antimycotics (containing 100 U/ml penicillin, 100 μg/ml streptomycin sulfate and 0.25 μg/ml amphotericin B) from Sigma. Multipotency of the mMSC was evaluated by adipogenic, osteogenic and chondrogenic differentiation. PC12SWQ8 cells were seeded in 6-cm Petri dishes (2×10^6 cells per dish) and cultured for 24 h under NCs. After 24 h, 3×10^5 mMSCs were added to PC12SWQ8 cultures. The monocultures of mMSC and PC12SWQ8 cells, as well as their co-cultures were in each case incubated in the presence or absence of EPO (5 U/ml) and under either normoxic or hypoxic culture conditions for 48 h. Thereafter, the respective cell culture supernatants were centrifuged ($350 \times g$, 8 min, 4°C) and frozen (−80°C) until the measurement of the cytokines by multiplex analysis, which was performed as described elsewhere.[45] Briefly, 50 μl medium from each dish was used for detection of interleukin-1 beta (IL-1β), IL-2, IL-4, IL-5, IL-6, IL-10, IL-12 (p70), GM-CSF, interferon-gamma (IFN-γ) and tumor necrosis factor-alpha (TNF-α). The quantification of these cytokines was performed with a Beadlyte Mouse Multi-Cytokine BeadmasterTM Kit (Upstate, Lake Placid, NY, USA) and a Luminex-100 system (Luminex Corporation, Austin, TX, USA), according to the manufacturer's instructions. The cytokine concentrations in the cell culture supernatants were extrapolated from their respective standard curves by 5-parameter logistic analysis.

Quantification of Abeta$_{1-42}$ in the cell culture supernatant of mMSC and rat APPsw-PC12 (PC12SWQ8) cells. For quantification of Abeta$_{1-42}$, 50 μl of the same cell culture supernatant as for the cytokine assay were taken and assayed with a highly sensitive enzyme-linked immunosorbent assay (hAmyloid β42 ELISA, The GENETICS Company, Zürich, Switzerland) according to the manufacturer's manual.

Immunofluorescence analyses. For the immunofluorescence studies, hMSCs (2.5×10^5) were grown under normoxic and hypoxic conditions in 60-mm cell culture dishes (BD Falcon, Heidelberg, Germany) containing coverslips. After fixation with −20°C cold methanol, the cells were rinsed with PBS and incubated with primary antibodies diluted in PBS for 1 h at RT. Dilutions of primary antibodies were as follows: anti-EPOR (1 : 50; rabbit polyclonal, Santa Cruz, Santa Cruz, CA, USA), anti-GFAP (1 : 10; mouse monoclonal, Progen, Heidelberg, Germany), anti-β-tubulin III clone TUJ1 (1 : 250, mouse monoclonal, R&D Systems), anti-GLAST (1 : 100, rabbit polyclonal, Abcam, Cambridge, UK), anti-EPO (1 : 75, mouse monoclonal, AbD Serotec, Oxford, UK), anti-synaptophysin (1 : 50, US Biological, rabbit polyclonal, Swampscott, MA, USA) or anti-GS (1 : 100, rabbit polyclonal, Sigma), or anti-human neuronal nuclei-specific protein (1 : 25, mouse monoclonal, Chemicon International, Nürnberg, Germany). The cells were washed twice with

PBS and incubated in the dark with the secondary antibodies, fluorescein isothiocyanate-conjugated goat anti-rabbit IgG (1 : 100) or goat anti-mouse IgG (1 : 100), and Cy3-conjugated goat anti-mouse IgG (1 : 800) or goat anti-rabbit IgG (1 : 800; all from Jackson ImmunoResearch, Newmarket, UK), for 1 h at RT. After washing twice with PBS containing 0.1% Triton X-100 (Sigma), samples were mounted with Vectashield medium (Vector Laboratories, Burlingame, CA, USA) containing DAPI and assessed by fluorescent microscopy.

Western blot analyses. Western blotting was carried out using protein lysates from 2.5×10^5 cells. Protein concentrations were measured using the Bradford assay. For each lane, 50 μg of proteins were subjected to SDS-PAGE in a 12.5% gel and transferred to PVDF membranes by tank blotting. Membranes were blocked in 0.66% (v/w) I-Block in PBS (Tropix, Applied Biosystems, Weiterstadt, Germany) for 1.5 h and were then incubated at 4°C overnight with antibodies against ChAT (1 : 1000, Biozol, Eching, Germany), synaptophysin (1 : 100, US Biological), Wnt3a (dilution 1 : 1000, Cell Signaling Technology, Frankfurt, Germany), leukemia-inhibitory factor (LIF, 1 : 200, Santa Cruz Biotechnology), EPO receptor (EPOR, 1 : 300, Santa Cruz Biotechnology, Heidelberg, Germany), neprilysin (1 : 1000, R&D systems), GLAST (1 : 5000, Chemicon International), β-catenin (1 : 1000, BD, BD Biosciences), GFAP mouse (dilution 1 : 1000, Progen) and GAPDH (1 : 1000, Chemicon International; loading control). For visualization of antibody binding, membranes were incubated for 2 h at RT with alkaline phosphatase-conjugated goat anti-rabbit or anti-mouse or rabbit anti-sheep or anti-guinea pig secondary antibodies (Tropix), diluted 1 : 10.000 in PBS and thereafter exposed to CDP-Star (Tropix) as chemoluminescence substrate for 1 h in the dark room. Signal intensities were recorded using a CCD camera system and sub-saturated images were analyzed semi-quantitatively by densitometry using the TINA software (version 2.09g, Raytest, Straubenhardt, Germany). Data were normalized to the respective densitometric values of normoxic controls and expressed as percent values.

GS activity assay. The cells (3×10^4 per well) were washed once with ice-cold PBS and lysed by adding 125 μl 50 mM imidazole/HCl buffer (pH 7.2). After a freezing–thawing cycle (-80°C to RT), 25 μl of the lysates were pipetted into a separate 96-well plate for protein determination. The remaining 100 μl lysates were used for the GS activity assay. GS was determined by measuring its γ-glutamyltransferase activity by following the formation of a complex between the reaction product γ-mono-hydroxamate and ferric chloride. The reaction was started by addition of 100 μl of reaction mixture (50 mM imidazole/HCl buffer pH 7.2, 2 mM MnCl$_2$, 25 mM sodium arsenate, 0.16 mM ADP, 50 mM L-glutamine and 25 mM NH$_2$OH · HCl) and incubated at 37°C for 2 h. The reaction was stopped by adding 400 μl stop solution consisting of 0.37 M FeCl$_3$, 0.67 M HCl and 0.2 M trichloroacetic acid. Precipitated proteins were removed by centrifugation at $15000 \times g$ (5 min, 4°C) and the absorbance of the supernatant was measured at 540 nm. Ten standards of γ-mono-hydroxamate dissolved in lysis buffer were prepared in the range of 0–5 μmol and treated equally. Activity of GS was determined based on a standard value of 1 U as the amount of the enzyme required for generation of 1 μmol γ-mono-hydroxamate/min. The raw data expressed in U/mg protein were normalized against the respective normoxic or hypoxic control in the presence or absence of 1 mM Glu and expressed as percentages.

Preparation of cDNA and quantification by real-time PCR. Mesenchymal stem cell total RNA was extracted from hMSCs by the RNeasy Mini Kit (Qiagen, Hilden, Germany). Except for the detection of β-tubulin III mRNA (see below), reverse transcription of total RNA was carried out with Superscript II and Oligo(dT) primers (Invitrogen). Total RNA (360 ng) was reverse transcribed in a 20 μl reaction and 1 μl of this reaction was subjected to qPCR, using the Platinum-SYBR Green$^{\rightarrow}$ qPCR Supermix (Invitrogen), 0.6 μM forward (sense, s) and reverse (antisense, as) primers and 100 nM ROX. Oligonucleotide primers for different genes were designed with the Primer3 software (http://frodo.wi.mit.edu/cgi-bin/primer3/primer3_www.cgi). The primers used for qPCR are listed in Table 3.

For the muscarinic receptors, primers were chosen within the coding exon to ensure quantification of all transcripts (muscarinic receptor presents different splice variants in the 5′ UTR). To control genomic contamination of the mRNA preparation, three additional sense primers, matching to intronic regions of the muscarinic receptor genes (marked by an asterisk) were used in combination with the respective antisense primer in the qPCR. For β_2-microglobulin and NGF transcript amplification, intron-flanking primers were used.

Table 3 Primer sequences for qPCR

Gene	Direction	5′–3′ sequence
M1R	S	TGCTGACCTCATCATCGGTA
	As	CGGAGAAGTAGCGGTCAAAGC
	s*	TCCACTTATGGCTGGGAAAG
M2R	S	GGCCATTCCAAAGATGAGAA
	As	ACAATCTTGCGGGCTACAATATT
	s*	GGCTCTGGTACTTGCAGCTC
M3R	S	GCCTGTGCCGATCTGATTAT
	As	GGCCTCGTGATGGAAAAGTA
	s*	AGAAATGAGAAAAATGTGGGAAAA
β_2-microglobulin	S	TTTCATCCATCCGACATTGA
	As	CCTCCATGATGCTGCTTACA
NGF	S	TCCGGACCCAATAACAGTTT
	As	CAGTGTCAAGGGAATGCTGA

Except in the case of β-tubulin III (see below), PCR was carried out in an MX 3000P instrument (Stratagene, La Jolla, CA, USA) using the following protocol: 2 min at 50°C, 2 min at 95°C, and 50 cycles of 15 s at 95°C and 30 s at 60°C. Threshold cycle (c_T) values were set within the exponential phase of PCR and normalization was performed to β_2-microglobulin for each sample to generate Δc_T values. A product melting curve was recorded to confirm a single amplicon. The correct product size was verified by agarose gel electrophoresis. The extracted total RNA and the qPCR reaction were tested for genomic contamination (additional primers annealing in intron regions listed in the Table 3). There was no significant genomic contamination in any RNA preparation.

Quantification of β-tubulin III mRNA in hMSC. For the determination of β-tubulin III mRNA by qPCR, 500 ng of total RNA was reverse transcribed with AMV reverse transcriptase (PEQ-Lab, Erlangen, Germany), random primers (Promega) and oligo(dT)15 primer (Promega). Real-time PCR assays were carried out using the LightCycler FastStart DNA Master SYBR Green I system (Roche, Mannheim, Germany) in the Light Cycler 2.0 instrument. PCR was carried out with 2 μl of reverse transcriptase product in 10 μl PCR mix for a total of 45 cycles. After 10 min at 95°C for polymerase activation, 45 cycles of PCR followed (denaturation at 95°C for 5 s, annealing at 63°C for 10 s, extension at 72°C for 9 s). A melting curve analysis was subsequently carried out to confirm the presence of a uniform PCR product. The primers used were 5′-CCA TTC TGG TGG ACC TGG AGC CTG GAA-3′ (sense) and 5′-GCT GGA AGC CCT GCA GGC AGT CAC AAT-3′ (antisense). The data are shown as relative expression ratios with respect to the mean of the normoxic control.

Calcium imaging. The function of MSC ACh receptors was analyzed by calcium imaging using a Zeiss Axioskop (Carl Zeiss AG, Jena, Germany) equipped with an imaging system from Visitron Systems (Puchheim, Germany) and the Metafluor 6.2 imaging software (Universal Imaging/Molecular Devices, Downingtown, PA, USA). hMSC from hypoxic controls (48 h incubation under HC) and those treated with EPO (5 U/ml) under hypoxia for 48 h were loaded with the Ca^{2+}-sensitive fluorescent dye, Fura-2, by incubation with a solution containing 150 mM NaCl, 5 mM KCl, 2 mM CaCl$_2$, 2 mM MgCl$_2$, 10 mM HEPES, 30 mM glucose and 2 μM fura-2 acetoxymethyl ester, and 0.04% Pluronic for 20–30 min at 37°C. Fluorescence was recorded before and after exposure to ACh (Sigma). The final ACh concentration in the bath solution was 10 μM. In control experiments, the muscarinic ACh antagonist atropine sulfate (Sigma) was used at a concentration of 500 nM.

Statistical analyses. All data presented in this study on hMSC obtained from five different donors were analyzed by Student's t-test for single comparisons and one-way ANOVA with Bonferroni test for multiple comparisons. Experiments were carried out separately on each of the five patient samples (3–6 replicates from each patient sample per condition). Thereafter, all data were included into the statistical analyses. The data shown in the diagrams include the pooled data of separately analyzed experiments. One representative experiment was chosen for the figures showing western blots (Figure 7) with the respective densitometric analyses (Table 1) and immunofluorescence (Figures 2, 3, 5 and 6). The data are presented as means ± S.E.M.; $P<0.05$ was considered significant.

1. Kim SS, Yoo SW, Park TS, Ahn SC, Jeong HS, Kim JW et al. Neural induction with neurogenin1 increases the therapeutic effects of mesenchymal stem cells in the ischemic brain. *Stem Cells* 2008; **26**: 2217–2228; e-pub ahead of print 10 July 2008..
2. Honma T, Honmou O, Lihoshi S, Harada K, Houkin K, Hamada H. Intravenous infusion of immortalized human mesenchymal stem cells protects against injury in a cerebral ischemia model in adult rat. *Exp Neurol* 2006; **199**: 56–66.
3. Park HJ, Lee PH, Bang OY, Lee G, Ahn YH. Mesenchymal stem cells therapy exerts neuroprotection in a progressive animal model of Parkinson's disease. *J Neurochem* 2008; **107**: 141–151; e-pub ahead of print 28 July 2008.
4. Pacary E, Legros H, Valable S, Duchatelle P, Lecocq M, Petit E et al. Synergistic effects of CoCl(2) and ROCK inhibition on mesenchymal stem cell differentiation into neuron-like cells. *J Cell Sci* 2006; **119**: 2667–2678.
5. Webster NJ, Ramsden M, Boyle JP, Pearson HA, Peers C. Amyloid peptides mediate hypoxic increase of L-type Ca2+ channels in central neurones. *Neurobiol Aging* 2006; **27**: 439–445.
6. Lassmann H, Reindl M, Rauschka H, Berger J, Aboul-Enein F, Berger T et al. A new paraclinical CSF marker for hypoxia-like tissue damage in multiple sclerosis lesions. *Brain* 2003; **126**: 1347–1357.
7. Decker MJ, Jones KA, Solomon IG, Keating GL, Rye DB. Reduced extracellular dopamine and increased responsiveness to novelty: neurochemical and behavioral sequelae of intermittent hypoxia. *Sleep* 2005; **28**: 169–176.
8. Theus MH, Wei L, Cui L, Francis K, Hu X, Keogh C et al. In vitro hypoxic preconditioning of embryonic stem cells as a strategy of promoting cell survival and functional benefits after transplantation into the ischemic rat brain. *Exp Neurol* 2008; **210**: 656–670.
9. Tilleux S, Hermans E. Neuroinflammation regulation of glial glutamate uptake in neurological disorders. *J Neurosci Res* 2007; **85**: 2059–2070.
10. Gonzalez FF, McQuillen P, Mu D, Chang Y, Wendland M, Vexler Z et al. Erythropoietin enhances long-term neuroprotection and neurogenesis in neonatal stroke. *Dev Neurosci* 2007; **29**: 321–330.
11. Zhang J, Li Y, Cui Y, Chen J, Lu M, Elias SB, Chopp M. Erythropoietin treatment improves neurological funtional recovery in EAE mice. *Brain Res.* 2005; **1034**: 34–39.
12. Ehrenreich H, Fischer B, Norra C, Schellenberger F, Stender N, Stiefel M et al. Exploring recombinant human erythropoietin in chronic progressive multiple sclerosis. *Brain* 2007; **130**: 2577–2588.
13. Chong ZZ, Li F, Maiese K. Erythropoietin requires NF-kappaB and its nuclear translocation to prevent early and late apoptotic neuronal injury during beta-amyloid toxicity. *Curr Neurovasc Res* 2005; **2**: 387–399.
14. Xue YQ, Zhao LR, Guo WP, Duan WM. Intrastriatal administration of erythropoietin protects dopaminergic neurons and improves neurobehavioral outcome in a rat model of Parkinson's disease. *Neuroscience* 2007; **146**: 1245–1258.
15. Danielyan L, Mueller L, Proksch B, Kabisch D, Weller M, Wiesinger H et al. Similar protective effects of BQ-123 and erythropoietin on survival of neural cells and generation of neurons upon hypoxic injury. *Eur J Cell Biol* 2005; **84**: 907–913.
16. Esneault E, Pacary E, Eddi D, Freret T, Tixier E, Toutain J et al. Combined therapeutic strategy using erythropoietin and mesenchymal stem cells potentiates neurogenesis after transient focal cerebral ischemia in rats. *J Cereb Blood Flow Metab* 2008; **28**: 1552–1563.
17. Kemp CR, Willems E, Wawrzak D, Hendrickx M, Agbor Agbor T, Leyns L. Expression of Frizzled5, Frizzled7, and Frizzled10 during early mouse development and interactions with canonical Wnt signaling. *Dev Dyn* 2007; **236**: 2011–2019.
18. Zwezdaryk KJ, Coffelt SB, Figueroa YG, Liu J, Phinney DG, LaMarca HL et al. Erythropoietin, a hypoxia-regulated factor, elicits a pro-angiogenic program in human mesenchymal stem cells. *Exp Hematol* 2007; **35**: 640–652.
19. Robinson SR. Neuronal expression of glutamine synthetase in Alzheimer's disease indicates a profound impairment of metabolic interactions with astrocytes. *Neurochem Int* 2000; **36**: 471–482.
20. de Hemptinne I, Vermeiren C, Maloteaux JM, Hermans E. Induction of glial glutamate transporters in adult mesenchymal stem cells. *J Neurochem* 2004; **91**: 155–166.
21. Habler OP, Messmer KF. The physiology of oxygen transport. *Transfus Sci* 1997; **18**: 425–435.
22. Harrison JS, Rameshwar P, Chang V, Bandari P. Oxygen saturation in the bone marrow of healthy volunteers. *Blood* 2002; **99**: 394.
23. Dings J, Meixensberger J, Jager A, Roosen K. Clinical experience with 118 brain tissue oxygen partial pressure catheter probes. *Neurosurgery* 1998; **43**: 1082–1095.
24. Tsang SW, Pomakian J, Marshall GA, Vinters HV, Cummings JL, Chen CP et al. Disrupted muscarinic M1 receptor signaling correlates with loss of protein kinase C activity and glutamatergic deficit in Alzheimer's disease. *Neurobiol Aging* 2007; **28**: 1381–1387.
25. Caccamo A, Oddo S, Billings LM, Green KN, Martinez-Coria H, Fisher A et al. M1 receptors play a central role in modulating AD-like pathology in transgenic mice. *Neuron* 2006; **49**: 671–682.
26. Henry-Feugeas MC. Alzheimer's disease in late-life dementia: a minor toxic consequence of devastating cerebrovascular dysfunction. *Med Hypotheses* 2008; **70**: 866–875.
27. Hoogduijn MJ, Cheng A, Genever PG. Functional nicotinic muscarinic receptors on mesenchymal stem cells. *Stem Cells Dev* 2008; **18**: 103–112.
28. Zhu X, Birnbaumer L. G protein subunits and the stimulation of phospholipase C by Gs-and Gi-coupled receptors: lack of receptor selectivity of Galpha(16) and evidence for a synergic interaction between Gbeta gamma and the alpha subunit of a receptor activated G protein. *Proc Natl Acad Sci USA* 1996; **93**: 2827–2831.
29. Arien-Zakay H, Nagler A, Galski H, Lazarovici P. Neuronal conditioning medium and nerve growth factor induce neuronal differentiation of collagen-adherent progenitors derived from human umbilical cord blood. *J Mol Neurosci* 2007; **32**: 179–191.
30. Walton RM, Wolfe JH. In vitro growth and differentiation of canine olfactory bulb-derived neural progenitor cells under variable culture conditions. *J Neurosci Methods* 2008; **169**: 158–167.
31. Katoh M. WNT signaling in stem cell biology and regenerative medicine. *Curr Drug Targets* 2008; **9**: 565–570.
32. Slevin M, Krupinski J, Mitsios N, Perikleous C, Cuadrado E, Montaner J et al. Leukaemia inhibitory factor is over-expressed by ischaemic brain tissue concomitant with reduced plasma expression following acute stroke. *Eur J Neurol* 2008; **15**: 29–37.
33. Lim JH, Chun YS, Park JW. Hypoxia-inducible factor-1alpha obstructs a Wnt signaling pathway by inhibiting the hARD1-mediated activation of beta-catenin. *Cancer Res.* 2008; **68**: 5177–5184.
34. Farías GG, Godoy JA, Hernández F, Avila J, Fisher A, Inestrosa NC. M1 muscarinic receptor activation protects neurons from beta-amyloid toxicity. A role for Wnt signaling pathway. *Neurobiol Dis* 2004; **17**: 337–348.
35. de Boer J, Siddappa R, Gaspar C, van Apeldoorn A, Fodde R, van Blitterswijk C. Wnt signaling inhibits osteogenic differentiation of human mesenchymal stem cells. *Bone* 2004; **34**: 818–826.
36. Bisaglia M, Venezia V, Piccioli P, Stanzione S, Porcile C, Russo C et al. Acetaminophen protects hippocampal neurons and PC12 cultures from amyloid beta-peptides induced oxidative stress and reduces NF-kappaB activation. *Neurochem Int* 2002; **41**: 43–54.
37. Patel NS, Paris D, Mathura V, Quadros AN, Crawford FC, Mullan MJ. Inflammatory cytokine levels correlate with amyloid load in transgenic mouse models of Alzheimer's disease. *J Neuroinflammation* 2005; **11**: 1–9.
38. Strunk T, Härtel C, Temming P, Matzke N, Zimmer J, Schultz C. Erythropoietin inhibits cytokine production of neonatal and adult leukocytes. *Acta Paediatr* 2008; **97**: 16–20.
39. Kumral A, Baskin H, Yesilirmak DC, Ergur BU, Aykan S, Genc S et al. Erythropoietin attenuates lipopolysaccharide-induced white matter injury in the neonatal rat brain. *Neonatology* 2007; **92**: 269–278.
40. Volmar CH, Ait-Ghezala G, Frieling J, Paris D, Mullan MJ. The granulocyte macrophage colony stimulating factor (GM-CSF) regulates amyloid beta (Abeta) production. *Cytokine* 2008; **42**: 336–344.
41. Iwata N, Tsubuki S, Takaki Y, Shirotani K, Lu B, Gerard NP et al. Metabolic regulation of brain Abeta by neprilysin. *Science* 2001; **292**: 1550–1552.
42. Colter DC, Sekiya I, Prockop DJ. Identification of a subpopulation of rapidly self-renewing and multipotential adult stem cells in colonies of human marrow stromal cells. *Proc Natl Acad Sci USA* 2001; **98**: 7841–7845.
43. Schäfer R, Dominici M, Muller I et al. Progress in characterization, preparation and clinical applications of non-hematopoietic stem cells, 29–30 September 2006, Tubingen, Germany. *Cytotherapy* 2007; **9**: 397–405.
44. Kern S, Eichler H, Stoeve J, Kluter H, Bieback K. Comparative analysis of mesenchymal stem cells from bone marrow, umbilical cord blood or adipose tissue. *Stem Cells* 2006; **24**: 1294–1301.
45. Danielyan L, Lourhmati A, Verleysdonk S, Kabisch D, Proksch B, Thiess U et al. Angiotensin receptor type 1 blockade in astroglia decreases hypoxia-induced cell damage and TNF alpha release. *Neurochem Res* 2007; **32**: 1489–1498.

Supplementary Information accompanies the paper on Cell Death and Differentiation website (http://www.nature.com/cdd)